The Winthrop McNair Research Bulletin

Volume 1 *The Winthrop McNair Research Bulletin Volume 1*

Article 15

2015

Synthesis and evaluation of symmetrical biphenyltetrols as aggregation inhibitors for Alzheimer's amyloid-β peptide

Sarah L. Wicks
Winthrop University, wickss2@winthrop.edu

James M. Hanna
Winthrop University, hannaj@winthrop.edu

Robin Lammi
Winthrop University, lammir@winthrop.edu

Synthesis and evaluation of symmetrical biphenyltetrols as aggregation inhibitors for Alzheimer's amyloid-β peptide

Sarah L. Wicks
James M. Hanna, Jr., Ph.D. (Mentor)
Robin K. Lammi, Ph.D. (Mentor)
Funding: Winthrop University McNair Scholars Program and an NIH-INBRE grant from the National Center for Research Resources and the National Institute for General Medical Sciences.

ABSTRACT

Inhibiting the aggregation of amyloid-beta peptide (Aβ) is one therapeutic target for the prevention and treatment of Alzheimer's disease. We have previously demonstrated that biphenyl-3,3',4,4'-tetrol (3,4-BPT) effectively abrogates Aβ aggregation at stoichiometric concentrations. To investigate molecular architecture and determine how the positioning of the hydroxyl hydrogen-bond donors impacts inhibitor efficacy, we have synthesized four additional symmetrical biphenyltetrols (2,3-, 2,4- 2,5- and 3,5-BPT). We have evaluated these inhibitors by means of Congo red and Thioflavin T dye-binding assays to monitor Aβ aggregation as a function of time and to determine inhibitor IC50 values for reducing equilibrium levels of aggregation. 2,3- and 2,5-BPT were observed to be promising inhibitors of Aβ aggregation: we have qualitatively assessed their IC50 values to be approximately 7X and 3-4X, respectively. In contrast, 2,4- and 3,5-BPT showed little to no inhibition. Thus, 2,5-BPT was the most successful of the four inhibitors evaluated, however; it was not as effective as 3,4-BPT, studied previously (IC50 = 1.0 ± 0.3X). The four isomers we have characterized exhibit a range of IC50 values spanning more than one order of magnitude, likely due to varying abilities to bind to A□ assemblies. Future work will involve further evaluation of the symmetrical biphenyltetrols, by methods including circular dichroism and transmission electron microscopy, which will afford greater insight into the Aβ assemblies formed in the presence and absence of inhibitors. These results will aid in the rational design of additional small-molecule aggregation inhibitors, including unsymmetrical biphenyltetrols and other architectures bearing hydroxyl substituents in those positions associated with the greatest inhibitory efficacy.

INTRODUCTION

Alzheimer's disease (AD) is currently the sixth-leading cause of death in the United States.[1] The aggregation of amyloid-β (Aβ), a peptide composed of 39-43 amino acids that is formed via proteolytic cleavage of the amyloid precursor protein (APP), is strongly linked to Alzheimer's disease (AD).[2] Monomeric Aβ self-assembles to form an array of neurotoxic, β-structured aggregates, including soluble oligomers and insoluble fibrils. The fibrils have received great attention as the primary component of extracellular senile plaques characteristic of AD brain.[3] Research efforts in the last 10-15 years have shown that smaller Aβ assemblies, specifically soluble oligomers, are more neurotoxic than insoluble fibrils.[4] Therefore, the inhibition of Aβ aggregation is one therapeutic target for the prevention and treatment of AD.

Previous research has hypothesized that small molecules can be designed and synthesized to bind to and inhibit the aggregation of Aβ. A number of small molecules containing oxygenated aromatic rings have demonstrated varying degrees of inhibitory activity.[5,6] Reinke and Gestwicki previously evaluated curcumin (**Figure 1**) and curcumin-like molecules to identify structural features that are important for inhibition.[7] They identified three major characteristics thought to be necessary for the inhibition of Aβ aggregation: 1) two aromatic groups, 2) one or more polar, hydrogen bonding substituents, and 3) a rigid linker of 8-16 Å.[7]

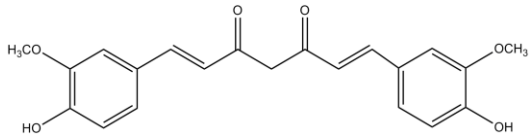

Figure 1. Curcumin

To increase understanding of the structure-activity relationship between curcumin-related molecules and Aβ inhibition, we previously synthesized and evaluated three isomeric tetrahydroxyterphenyls and a tetrahydroxybiphenyl.[8] The terphenyls (3,3'',4,4''-*tetrahydroxy*-o-*terphenyl*, 3,3'',4,4''-*tetrahydroxy*-m-*terphenyl*, and 3,3'',4,4''-*tetrahydroxy*-p-*terphenyl*) were synthesized with the geometry around the phenyl linker in the *ortho*- (OTT), *meta*- (MTT), and *para*- (PTT) positions, respectively (**Figure 2**). These compounds were expected to inhibit Aβ aggregation because they contained two hydroxy-substituted aromatic groups connected by a rigid linker, in agreement with the structural features identified by Reinke and Gestwicki.

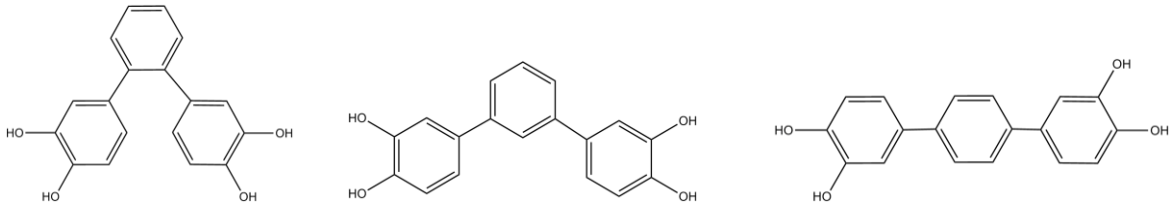

Figure 2. Representative isomers of terphenyl-3,3",4,4"-tetrol (OTT, MTT, and PTT, respectively)

The biphenyltetrol was synthesized to evaluate the need for the phenyl linker because, according to Reinke and Gestwicki, the molecule should fail to inhibit Aβ aggregation. All molecules were evaluated by means of a Congo red assay at a 10X concentration (1X = 25μM). Surprisingly, Stevens and coworkers concluded that 3,3',4,4'-biphenyltetrol (3,4-BPT) was the most successful inhibitor with an IC_{50} value near 1.0X.[8] These researchers suggested that the biphenyltetrol is more conformationally restricted than the inhibitors that were included in the Reinke and Gestwicki study; therefore, the characteristics Reinke and Gestwicki associated with inhibitory efficacy may not apply.

3,4-BPT effectively abrogates Aβ aggregation at stoichiometric concentrations. This promising result inspired us to investigate this molecular architecture and determine how the positioning of hydroxyl hydrogen-bond donors impacts inhibitor efficacy. Toward that goal, we aimed to synthesize and evaluate five isomers of 3,4-BPT (**Figure 3**). The interaction occurring between monomeric Aβ and BPT is thought to be through hydrogen bonding; however, the mechanism is relatively unknown. The rearrangement of the hydroxyls around the aromatic rings will aid in determining which positions are most favorable for inhibition. Currently, we have synthesized and characterized 2,3-, 2,4-, 2,5-, and 3,5-BPT. There have been limitations in synthesizing 2,6-BPT, in which steric hindrance is thought to be preventing the formation of the required intermediate; however, the complete synthesis of 2,6-BPT is currently in progress.

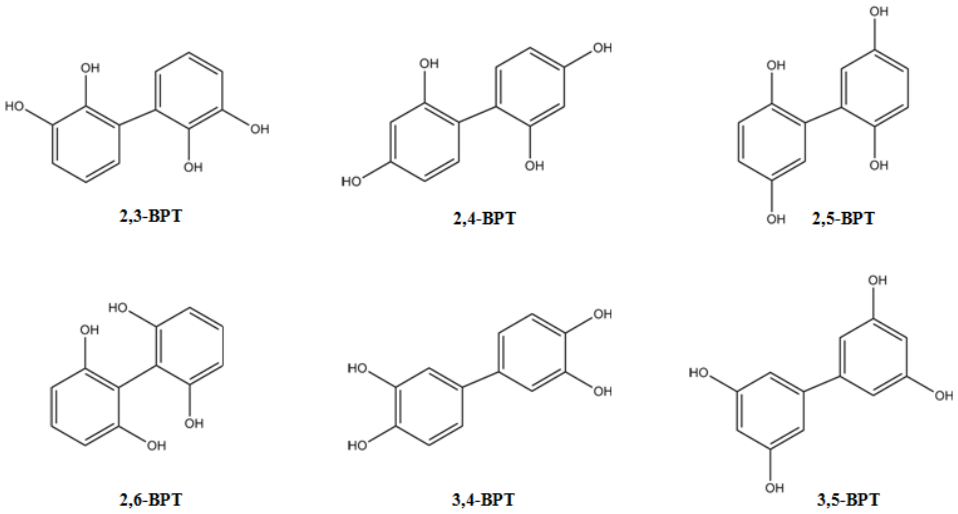

Figure 3. Structures of biphenyl-2,2',3,3'-tetrol (2,3-BPT), biphenyl-2,2',4,4'-tetrol (2,4-BPT), biphenyl-2,2',5,5'-tetrol (2,5-BPT), biphenyl 2,2',6,6'-tetrol (2,6-BPT), biphenyl-3,3',4,4'-tetrol (3,4-BPT), and biphenyl-3,3',5,5'-tetrol (3,5-BPT), respectively.

The four isomeric compounds were evaluated by means of Thioflavin T and Congo red dye-binding assays. The dyes selectively bind β-sheet structures and allow Aβ aggregation to be monitored as a function of time for samples with and without inhibitor. We have employed Congo red assays to determine inhibitor IC_{50} values and thus quantify the efficacy of the symmetrical molecules. When the evaluation is complete, we expect to report a range of inhibitor IC_{50} values that will support our hypothesis that hydroxyl positioning has a measurable effect on inhibitor activity. These results may impact the rational design of future inhibitors.

METHODS

Disaggregation of Aβ

Lyophilized Aβ(1-40) peptide was purchased from AnaSpec, Inc. and stored at -20 °C. The peptide was brought to room temperature and dissolved in hexafluoroisopropnal (HFIP), resulting in a peptide concentration of 5 mg/mL. The vial was sealed to prevent evaporation loss and remained in a hood overnight. The following day, HFIP was evaporated under nitrogen for at least 1 hour, leaving behind a peptide film. The film was dissolved and thoroughly mixed in dimethyl sulfoxide (DMSO) for 20 minutes to obtain a final peptide concentration of 2 mM. Aliquots of the peptide solution were transferred to microcentrifuge tubes and stored in a -80 °C freezer.

Thioflavin T (ThT) Assay

Aβ(1-40) aliquots in DMSO were brought to room temperature and diluted to 50 μM with 25 mM phosphate buffer solution (25 mM sodium phosphate, 120 mM NaCl, 1.25 μM Thioflavin T, and 0.02% sodium azide, pH 7.4) maintaining 10% DMSO by volume. Inhibitor samples were prepared similarly with the addition of a biphenyltetrol, 10 mM in DMSO, at varying volumes to obtain the desired inhibitor concentration (0-500 μM, i.e., 0-10X). Samples with and without inhibitor were incubated at 37 °C and shaken at 1500 RPM to promote aggregation. Each sample was removed from the incubator/shaker periodically and loaded into a 1-cm path length quartz cuvette. Fluorescence spectra were acquired with an excitation wavelength of 450 nm and emission wavelengths of 460-600 nm. Samples were returned to the incubator/shaker and the cuvette was rinsed between samples 3 times with distilled water. The peak areas from the ThT spectra were integrated and plotted as a percentage of the control sample as a function of time.

Congo Red (CR) Assay

Aβ(1-40) aliquots in DMSO were brought to room temperature and diluted to 50 µM with phosphate buffered saline, (PBS, 1X concentration: 137 mM NaCl, 2.7 mM KCl, 4.3 mM Na_2HPO_4, and 1.47 mM KH_2PO_4, pH 7.4) maintaining 10% DMSO by volume. Inhibitor samples were prepared similarly with the addition of a biphenyltetrol, 10 mM in DMSO, at varying volumes to obtain the desired inhibitor concentration (0-500 µM, i.e., 0-10X). A CR stock solution of 50 µM was made in 1X PBS. Samples with and without inhibitor were incubated at 37 °C and shaken at 1500 RPM to promote aggregation. An aliquot of sample was removed from the incubator/shaker periodically and combined with an equal volume of 50 µM CR, diluting the CR and Aβ concentrations to 25 µM each. The CR/sample solution was mixed 20 times to ensure proper association between CR and Aβ and loaded in a 1-cm path length quartz cuvette; the absorbance was measured at the wavelengths of 403 and 541 nm. Between samples, the cuvette was rinsed 3 times with a 90% 1X PBS/10% DMSO solution. The concentrations of bound complex ([CR-Aβ]) for each sample, used to monitor Aβ aggregation, were calculated from the absorbance values and extinction coefficients at the measured wavelengths, according to Eq. 1.[9] The [CR-Aβ] for each sample was monitored and plotted as a function of time.

$$[\text{CR-A}\beta] = (A_{541}/47{,}800) - (A_{403}/38{,}100) \quad (1)$$

IC_{50} Determination

A range of inhibitor concentrations were evaluated to determine the overall inhibitory efficacy of each biphenyltetrol. Inhibitor samples were prepared as described above, with the desired BPT concentrations ranging from 25 µM to 500 µM (0.5X-10X). Control and inhibitor samples were incubated at 37 °C and shaken at 1500 RPM to promote aggregation. When aggregation of the control reached equilibrium, aliquots of the various inhibitor samples were taken in random order to measure [CR-Aβ]. Collecting data at equilibrium is favorable for the day-to-day reproducibility of results. Inhibitor concentrations were quantitatively compared by calculating respective [CR-Aβ] values as a percent of control. These responses were plotted versus the inhibitor concentration on a semi-log plot. The IC_{50} is the concentration at which aggregation is inhibited by 50 %.

RESULTS & DISCUSSION

Our preliminary data from the spectroscopic evaluations of four symmetrical biphenyltetrols show 2,4- and 3,5-BPT to be poor inhibitors of Aβ aggregation, while 2,3- and 2,5-BPT inhibit equilibrium levels of aggregation to a quantifiable degree. ThT and CR results were consistent, which allowed for verification of inhibitor efficacy by two methods and ensured accurate data collection.

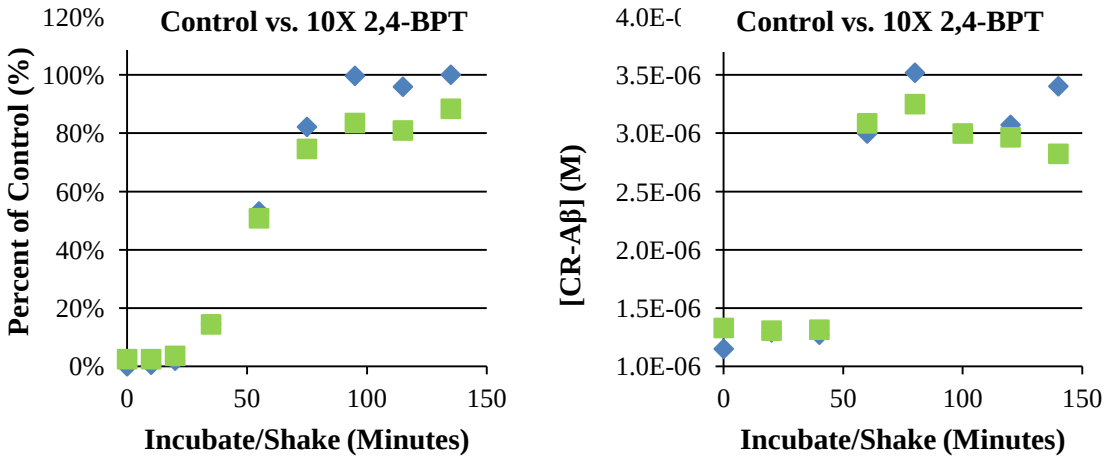

Figure 4. ThT (left) and CR (right) assay results for control vs. 10X 2,4-BPT

The ThT and CR data for 2,4-BPT at 10X concentration, **Figure 4**, illustrate the consistency of results between assays. At equilibrium, there is little difference between the control and 2,4-BPT samples, which indicates little to no inhibition.

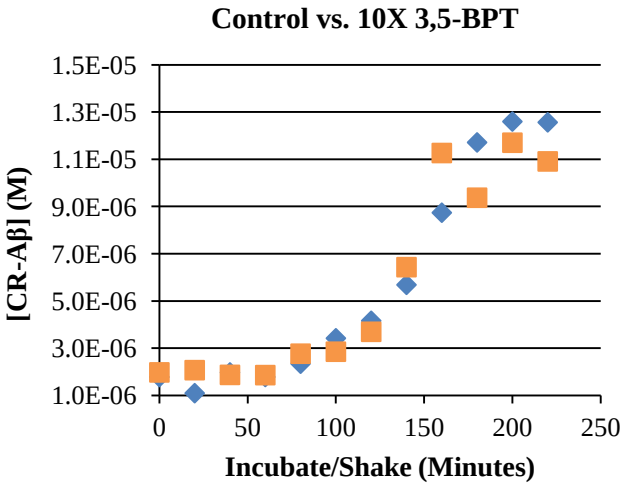

Figure 5. Congo red assay results for 3,5-BPT (10X concentration, squares) versus inhibitor-free control (diamonds). At 10X, 3,5-BPT demonstrates little inhibitory activity against Aβ aggregation.

We saw similar results with 3,5-BPT, **Figure 5**, where there is little difference between the control and 3,5-BPT samples at equilibrium. At 10X concentration, neither 2,4- nor 3,5-BPT demonstrate inhibitory properties against Aβ aggregation.

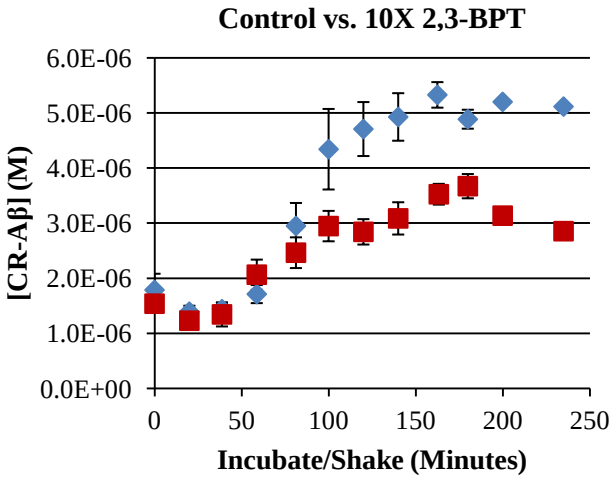

Figure 6. Congo red assay results for 2,3-BPT (10X, squares) versus inhibitor-free control (diamonds). In the presence of 10X 2,3-BPT, less CR-Aβ complex is formed, indicating some degree of inhibition.

There is a greater difference, at equilibrium, between the control and 10X 2,3-BPT samples which indicates some degree of inhibition (**Figure 6**). Similar results were seen with 10X 2,5-BPT in which the molecule demonstrated inhibitory properties against Aβ aggregation (**Figure 7**).

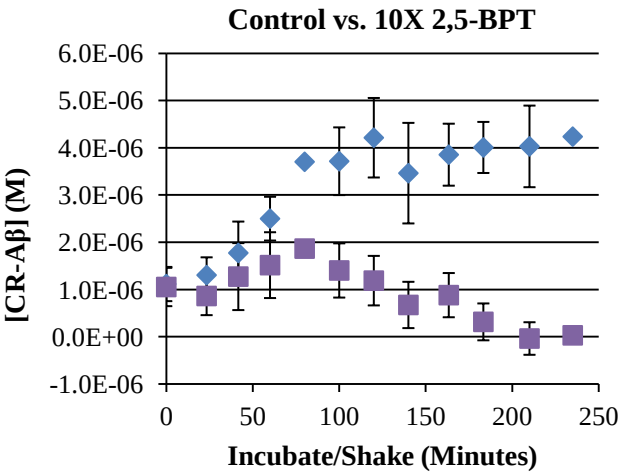

Figure 7. Congo red assay results for 2,5-BPT (10X, squares) show much less CR-Aβ formation compared to the control (diamonds), which indicates significant inhibition.

We can conclude from our preliminary data that altering the positions of the hydroxyl groups around the aromatic rings has an effect on inhibitor efficacy. We determined the 2,4- and 3,5- hydroxyl positions to be unfavorable for inhibition, whereas the 2,3- and 2,5- positions appear to be more favorable for hydrogen-bonding interactions with Aβ.

As a further evaluation of inhibitor efficacy, we investigated IC_{50} values for 2,3- and 2,5-BPT. From preliminary results, we qualitatively determined 2,3- and 2,5-BPT to have IC_{50} values of about 7X and 3-4X, respectively. Based on our previous ThT and CR results, the IC_{50} values of 2,4- and 3,5-BPT are expected to be greater than 10X. Thus, 2,5-BPT was the most effective inhibitor of the four molecules evaluated, but it did not match the efficacy of 3,4-BPT, for which the IC_{50} is 1.0 X.[3] The four isomers we have characterized exhibit a range of IC_{50} values spanning more than one order of magnitude, likely due to varying abilities to bind to Aβ assemblies. The range of inhibitory activity supports our hypothesis that altering positions of the hydroxyl groups affects inhibitor efficacy.

Future work will involve further evaluation of these symmetrical biphenyltetrols, by methods including circular dichroism and transmission electron microscopy, which will afford greater insight into the Aβ assemblies formed in the presence and absence of inhibitors. As a result of knowledge gained from preliminary studies of symmetrical biphenyltetrols, we have also synthesized two unsymmetrical biphenyltetrols, in which the hydroxyl groups occupy different positions on each ring (**Figure 8**): a hybrid of 3,4- and 2,3-BPT (biphenyl-2,3',4',3-tetrol, 3,4,2,3-BPT) as well as a hybrid of 3,4- and 2,5-BPT (biphenyl-2,3',4',5-tetrol, 3,4,2,5-BPT). These molecules will allow us to evaluate how the change in positioning of hydroxyl hydrogen-bond donors around the phenyl rings impacts inhibitor efficacy against Aβ aggregation.

Figure 8. Structures of biphenyl-2,3',4',3-tetrol (3,4,2,3-BPT, left) and biphenyl-2,3',4',5-tetrol (3,4,2,5-BPT, right)

REFERENCES

(1) 2013 Alzheimer's disease facts and figures; Alzheimer's Association: Chicago, IL, 2013.

(2) Kang, J.; Lemaire, H. G.; Unterbeck, A.; Salbaum, J. M.; Masters, C. L.; Grzeschik, K. H.; Multhaup, G.; Beyreuther, K.; Muller-Hill, B. The precursor of Alzheimer's disease amyloid A4 protein resembles a cell-surface receptor. *Nature*. **1987**, *325*, 733-736.

(3) Cras, P.; Kawai, M.; Lowery, D.; Gonzalez-DeWhitt, P.; Greenberg, B.; Perry, G. Senile plaque neuritis in Alzheimer disease accumulate amyloid precursor protein. *Proc. Natl. Acad. Sci.* **1991**, *88*, 7552-7556.

(4) Dahlgren, K. N.; Manelli, A. M.; Stine, W. B.; Baker, L. K.; Krafft, G. A.; LaDu, M. J. Oligomeric and fibrillar species of amyloid-beta peptides differentially affect neuronal viability. *J. Biol. Chem.* **2002**, *277*, 32046-32053.

(5) Churches, Q. I.; Caine, J.; Cavanagh, K.; Epa, V. C.; Waddington, L.; Tranberg, C. E.; Meyer, A. G.; Varghese, J. N.; Streltsov, V.; Duggan, P. J. Naturally occurring polyphenolic inhibitors of amyloid beta aggregation. *Bioorg. Med. Chem. Lett.* **2014**, *24*, 3108-3112.

(6) Yun, S. L.; Hye, Y. K.; YoungSoo, K.; Jae, H. S.; Eun, J. R.; Hogyu, H.; Kye, J. S. Small molecules that protect against β-amyloid-induced cytotoxicity by inhibiting aggregation of β-amyloid. *Bioorg. Med. Chem.* **2012**, *20*, 4921-4935.

(7) Reinke, A. A.; Gestwicki, J. E. Structure-activity relationships of amyloid beta-aggregation inhibitors based of curcumin: Influence of linker length and flexibility. *Chem. Biol. Drug. Des.* **2007**, *70*, 206-215.

(8) Stevens, C. B.; Hanna, J. M.; Lammi, R. K. Synthesis of tetrahydroxybiphenyls and tetrahydroxyterphenyls and their evaluation as amyloid-β aggregation inhibitors. *Bioorg. Med. Chem. Lett.* **2013**, *23*, 1703-1706.

(9) Klunk, W. E.; Jacob, R. F.; Mason, R. P. Quantifying amyloid β-peptide (Aβ) aggregation using the congo red-Aβ (CR-Aβ) spectrophotometric assay. *Anal. Biochem.* **1999**, *266*, 66-76.